九州大学大学院総合理工学府報告
第 45 巻 第 2 号 11-22 頁 令和 6 年 2 月

Engineering Sciences Reports, Kyushu University
Vol. 45, No. 2, pp. 11-22, FEB, 2024

Emission Spectra of He_2^* Excimer Produced from Ion-Ion Neutralization Reactions of He_2^+ with $C_6F_6^-$ and $C_6F_5Cl^-$ in the He Flowing Afterglow

Masaharu TSUJI*1,2† and Erika Oda−Sako*3
†E-mail of corresponding author: tsuji@cm.kyushu-u.ac.jp

(Received November 17, 2023, accepted December 1, 2023)

The ion-ion neutralization reactions of He_2^+ with $C_6F_6^-$ and $C_6F_5Cl^-$ were studied by observing He_2^* excimer emissions in the 200–990 nm region. He_2^* excimer emissions from six triplet states and six or five singlet states with excitation energies of 19.3−20.7 eV were identified in these two reactions. The relative formation rate constant of an upper u level of He_2^*, $k_0(u)$, rapidly decreased with increasing the excitation energy of He_2^*. Major triplet and singlet He_2^* states were the lowest observed $c^3\Sigma_g^+$ and $C^1\Sigma_g^+$ states, which occupied 70% and 21% of $\sum_u k_0(u)$, in the $He_2^+/C_6F_6^-$ reaction, and 69% and 18% in the $He_2^+/C_6F_5Cl^-$ reaction, respectively. The total formation ratios of triplet and singlet states were 78:22 in the $He_2^+/C_6F_6^-$ reaction and 81:19 in the $He_2^+/C_6F_5Cl^-$ reaction. No vibrational excitation was observed for all observed He_2^* states. The rotational distributions of $f^3\Sigma_u^+(v'=0)$, $e^3\Pi_g(v'=0)$, $d^3\Sigma_u^+(v'=0)$, $c^3\Sigma_g^+(v'=0)$, and $C^1\Sigma_g^+(v'=0)$ states were expressed by either single or double Boltzmann rotational temperatures of 310−1530 K. Rovibrational distributions of these excited states indicated that most of excess energies are not released as rovibrational energies of He_2^*, but they (90.4−97.2%) are deposited into relative translational energies of products and rovibrational energies of C_6F_5X (X=F, Cl). The observed vibrational and rotational distributions were compared with statistical ones assuming long lived $[He_2–C_6F_5X]^*$ intermediates.

Key words: *He_2^+ ion, Ion-Ion neutralization, Flowing afterglow, He_2^* excimer emission, Relative formation rate constant, Rotational temperature, Statistical prior distribution*

1. Introduction

Electron-ion and ion-ion recombination and neutralization processes are important loss processes of charged particles in space and man-made plasmas because of their extremely large cross sections due to long range Coulombic attractive forces between positive ions and electrons or negative ions.[1-6] In a preceding paper, we studied the formation of He_2^* excimer by three-body collisional radiative recombination (CRR) reaction (1) in the He flowing afterglow (FA):[7]

$$He_2^+ + e^- + e^- \rightarrow He_2^* + e^-. \quad (1)$$

Thirty triplet and twelve singlet transitions of He_2^* with excitation energies of 19.3–21.8 and 19.6–21.8 eV region, respectively, were identified. The relative formation rate constant of He_2^*, $k_0(u)$, rapidly decreased with increasing the excitation energy. Major triplet and singlet product He_2^* states were the lowest observed $c^3\Sigma_g^+$ and $C^1\Sigma_g^+$ states, which occupied 39.9% and 7.1% of $\sum_u k_0(u)$, respectively. The total intensity ratio of triplet and singlet states were 84:16 respectively. No vibrational excitation was observed for all thirty-four states. The rotational distributions of $f^3\Sigma_u^+(v'=0)$, $e^3\Pi_g(v'=0)$, and $d^3\Sigma_u^+(v'=0)$ were expressed by double Boltzmann rotational temperatures, whereas that of $c^3\Sigma_g^+(v'=0)$ was represented by a single Boltzmann temperature. On the basis of observed rovibrational distributions, most of the total excess energy (95.2−98.5%) is deposited into the relative translational energy of products. The observed vibrational and rotational

*1 Institute for Materials Chemistry and Engineering, and Research and Education Center of Green Technology
*2 Department of Molecular Science and Technology
*3 Department of Molecular Science and Technology, Graduate Student

distributions were lower than those of statistical prior ones calculated assuming a long lived $[He_2–e^-]^*$ intermediate. It was concluded that He_2^* molecules are not formed via long lived $[He_2–e^-]^*$ intermediate, where excess energies are statistically distributed to all degrees of freedom.

In the present study, the formation of He_2^* excimer by the ion-ion neutralization reactions of He_2^+ with $C_6F_6^-$ and $C_6F_5Cl^-$ are investigated using the He FA. The relative formation rate constants and rotational distributions of five typical states are determined. The observed vibrational and rotational distributions are compared with statistical ones assuming long lived $[He_2–C_6F_5X]^*$ (X=F, Cl) intermediates. Preliminary results of this paper have been communicated previously.[5,8]

2. Experimental

The FA apparatus used in this study has been previously described in detail.[5,8] In brief, $He(2^3S)$, He^+, and electrons were generated by a microwave discharge of high purity helium gas (Nippon Sanso, purity >99.995%) in a discharge flow operated at 1.6–1.8 Torr. The contribution of charged species to the observed emissions was examined by using a pair of ion-collector grids placed between the discharge section and the reaction zone.

The positive He_2^+ ions were formed by the three-body reaction of He^+ with 2He in a flow tube:

$$He^+ + 2He \xrightarrow{k_2} He_2^+ + He, \quad (2)$$

($k_2 = 8.3 \times 10^{-32}$ cm^6 molecule^{-2} s^{-1} [Ref. 9]).

An electron attachment gas, C_6F_6 (Tokyo Kasei, purity >99%) or C_6F_5Cl (Tokyo Kasei, >95%), was added from the first gas inlet placed 10 cm downstream from the center of microwave discharge, where negative $C_6F_6^-$ or $C_6F_5Cl^-$ ion was formed by a fast non-dissociative electron attachment to these two gases:

$$C_6F_6 + e^- \rightarrow C_6F_6^-, \quad (3)$$

($k_3 = 8.6 \times 10^{-8}$ cm^3 s^{-1} [Ref. 10]),

$$C_6F_5Cl + e^- \rightarrow C_6F_5Cl^-, \quad (4)$$

($k_4 = 1.0 \times 10^{-7}$ cm^3 s^{-1} [Ref. 11]).

The partial pressures of C_6F_6 and C_6F_5Cl in the reaction zone were 2−15 mTorr.

A reaction flame, observed around the C_6F_6 or C_6F_5Cl gas inlet was dispersed in the 200–1000 nm region with a Spex 1250M monochromator equipped with a cooled photomultiplier (Hamamatsu Photonics R376 or R316-02). The wavelength response of monochromator and the optical detection system were corrected using standard D_2 and halogen lamps.

3. Results and Discussion

3.1 Emission spectra of He_2^* excimer resulting from the $He_2^+/C_6F_6^-$ and $He_2^+/C_6F_5Cl^-$ ion-ion neutralization reactions

Figure 1 shows typical emission spectra in the 430–980 nm region resulting from the $He(2^3S)/C_6F_6$, He^+,He_2^+/C_6F_6, and He^+,$He_2^+/C_6F_6^-$ reactions. Figure 2 shows the corresponding spectra for C_6F_5Cl reagent. Six triplet and six or five singlet transitions of He_2^* given in Table 1 are identified in the $He_2^+/C_6F_6^-$ and $He_2^+/C_6F_5Cl^-$ reactions by referring to reported spectral data of He_2^*.[12-15] In addition to many He_2^* emissions, $C_6F_6^+(\tilde{B}–\tilde{X})$,[16] $C_6F_5Cl^+(\tilde{B}–\tilde{X})$,[17] He^*,[18] and H^*[18] emissions are observed. Strong broad $C_6F_6^+(\tilde{B}–\tilde{X})$ and $C_6F_5Cl^+(\tilde{B}–\tilde{X})$ emissions result from $He(2^3S)/C_6F_5X$ Penning ionization and He_2^+/C_6F_5X charge-transfer reactions.[19] He^* lines dominantly result from $He^+/C_6F_5X^-$ neutralization reactions.[19,20] H^* lines arise from reaction of $He(2^3S)$ with residual H_2O.[21]

The observed He_2^* emissions, on which the present work focuses, disappeared when charged species were removed from the He afterglow on applying an electrostatic potential to the grid. The formation of He_2(c, d, e, f, C, D, E, F) by the He_2^+/C_6F_6 and He_2^+/C_6F_5Cl charge-transfer reactions are highly endothermic,

Table 1. He_2^* emission systems produced $He_2^+/C_6F_6^-$ and $He_2^+/C_6F_5Cl^-$ reactions in the He FA.

Triplet transitions	Singlet transition
$f^3\Delta_u(3d\delta)$-$b^3\Pi_g$	$F^1\Delta_u(3d\delta)$-$B^1\Pi_g$
$f^3\Pi_u(3d\pi)$-$b^3\Pi_g$	$F^1\Pi_u(3d\pi)$-$B^1\Pi_g$
$f^3\Sigma_u^+(3d\sigma)$-$b^3\Pi_g$	$F^1\Sigma_u^+(3d\sigma)$-$B^1\Pi_g$
$e^3\Pi_g(3p\pi)$-$a^3\Sigma_u^+$	$E^1\Pi_g(3p\pi)$-$A^1\Sigma_u^+$
$d^3\Sigma_u^+(3s\sigma)$-$b^3\Pi_g$	$D^1\Sigma_u^+(3s\sigma)$-$B^1\Pi_g$[a]
$c^3\Sigma_g^+(3p\sigma)$-$a^3\Sigma_u^+$	$C^1\Sigma_g^+(3p\sigma)$-$A^1\Sigma_u^+$

a) Observed only in the $He_2^+/C_6F_6^-$ reaction.

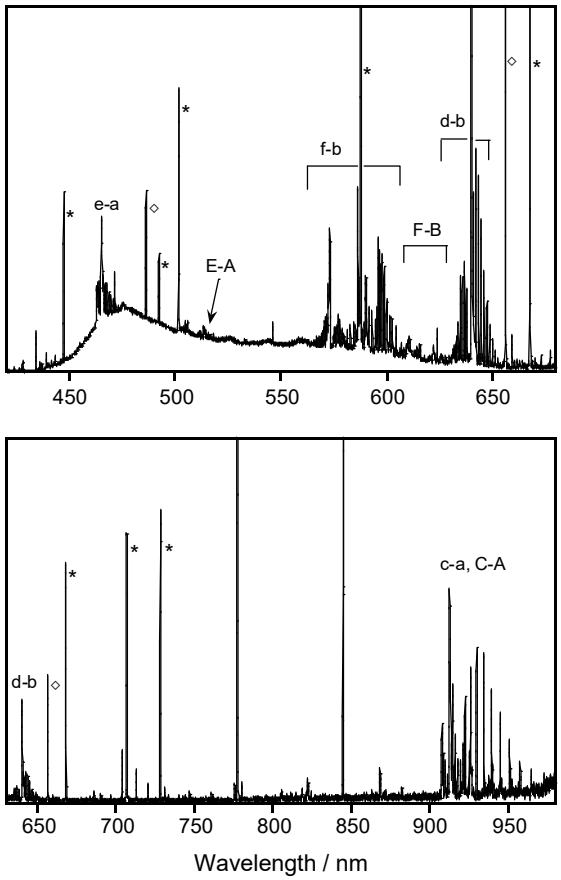

Fig. 1. Emission spectra of He_2* resulting from the $He_2^+/C_6F_6^-$ reaction in the He FA at a He gas pressure of 1.8 Torr. Lines marked by * and ◇ are He* and H* lines, respectively.

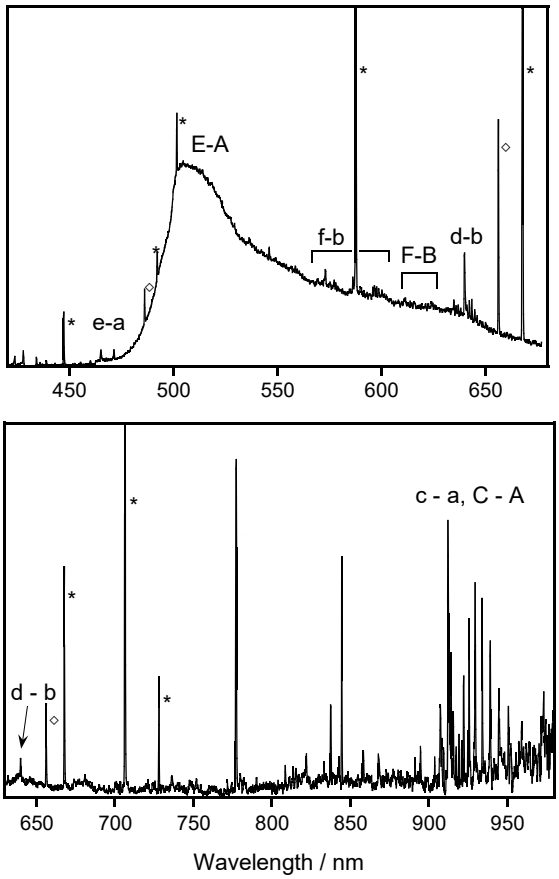

Fig. 2. Emission spectra of He_2* resulting from the $He_2^+/C_6F_5Cl^-$ reaction in the He FA at a He gas pressure of 1.8 Torr. Lines marked by * and ◇ are He* and H* lines, respectively.

because high energies are required for the ionization of C_6F_6 (9.90 eV) and C_6F_5Cl (9.72 eV):[22]

$$He_2^+ + C_6F_6 \rightarrow He_2(c\sim f,C\sim F) + C_6F_6^+ - (7.0\sim8.4\ eV), \quad (5)$$

$$He_2^+ + C_6F_5Cl \rightarrow He_2(c\sim f,C\sim F) + C_6F_5Cl^+ - (6.8\sim8.2\ eV). \quad (6)$$

Therefore, these processes can be energetically excluded from possible formation processes.

Figures 3 and 4 show energy-level diagrams of triplet and singlet states of He_2*, where observed emitting levels are shown in red. The excitation energies of He_2* and the recombination energy of He_2^+ (22.223 eV) were obtained from Ref. 12. We found that twenty-two triplet states and twelve singlet states of He_2* in the 19.3–21.8 eV region are formed in the $He_2^+/2e^-$ CRR reaction (1).[7] By the C_6F_6 or C_6F_5Cl addition to the He discharge flow, several He_2* bands with high excitation energies of 21.2–21.8 eV disappeared. On the other hand, six triplet levels from c to f states in the 19.3–20.7 eV region and six or five singlet levels from C to F states in the 19.6–21.3 eV region (Table 1 and Figs. 3 and 4) remained after C_6F_6 or C_6F_5Cl addition. These results indicate that electrons are completely scavenged by C_6F_6 or C_6F_5Cl, so that the contribution of CRR reaction (1) to the observed He_2* bands is negligible. Thus, remaining processes for the formation of He_2* are the following ion-ion neutralization reactions:

$$He_2^+ + C_6F_6^- \rightarrow He_2(c\sim f,C\sim F) + C_6F_6 + (0.97\sim2.4\ eV), \quad (7a)$$
$$\rightarrow He_2(c\sim f,C\sim F) + C_6F_5 + F - (2.7\sim4.1\ eV), \quad (7b)$$

$$He_2^+ + C_6F_5Cl^- \rightarrow He_2(c\sim f,C\sim F) + C_6F_5Cl + (0.75\sim2.2\ eV), \quad (8a)$$
$$\rightarrow He_2(c\sim f,C\sim F) + C_6F_5 + Cl - (1.8\sim3.2\ eV). \quad (8b)$$

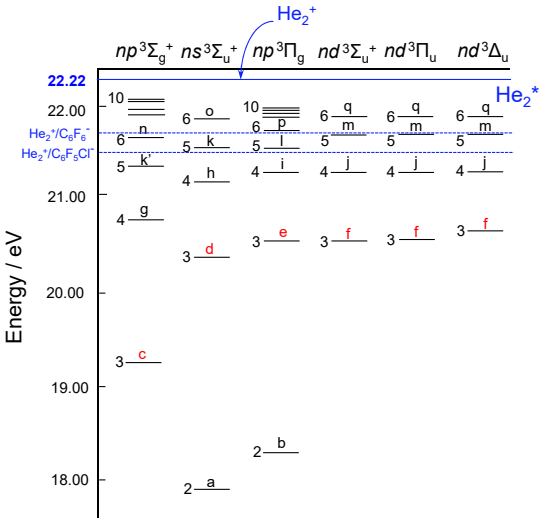

Fig. 3. Energy-level diagram of triplet states of He_2*. Observed emitting levels in the $He_2^+/C_6F_6^-$ and $He_2^+/C_6F_5Cl^-$ reactions are shown in red.

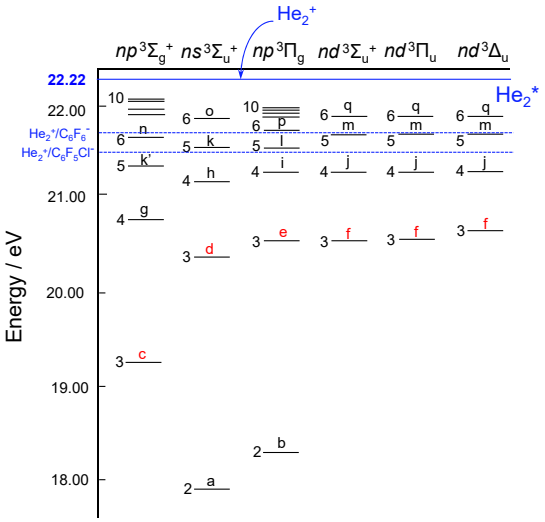

Fig. 4. Energy-level diagram of singlet states of He_2*. Observed emitting levels in the $He_2^+/C_6F_6^-$ and $He_2^+/C_6F_5Cl^-$ reactions are shown in red.

In processes (7a) and (8a), parent C_6F_5X molecules are formed as products, whereas C_6F_5 + X fragments are generated in processes (7b) and (8b). Electron affinities of C_6F_6 and C_6F_5Cl are 0.53 eV and 0.75 eV,[22] and dissociation energies of D(C_6F_5-F) and D((C_6F_5-Cl) are 5.03 eV and 3.97 eV, respectively.[23] By using these thermochemical data, $-\Delta H^o$ values for the formation of He_2(c~f,C~F) in processes (7a), (7b), (8a), and (8b) were estimated. Since the reactions (7b) and (8b) are endoergic, they can be excluded from possible reaction processes. The observation of He_2* states in the 19.3–20.7 eV region is consistent with the fact that processes (7a) and (8a) are responsible for the formation of He_2*. Based on above facts, it was concluded that He_2* states arise from neutralization reactions (7a) and (8a). The observed excited states in the $He_2^+/C_6F_5Cl^-$ reaction were the same as those in the $He_2^+/C_6F_6^-$ reaction except for the absence of the D state. This indicates that the difference in electron affinity between C_6F_6 and C_6F_5Cl does not affect the observed energy levels of He_2*.

3.2 Relative formation rate constants of He_2* in the $He_2^+/C_6F_6^-$ and $He_2^+/C_6F_5Cl^-$ reactions

Radiative lifetimes of the f, e, and d states have been measured as 19±5 ns, 25±5 ns, and, 57±10 ns, respectively.[24] Although the radiative lifetimes of the c, F, E, D, and C states observed in this study are unknown, they may be the same order as the above states. Radiative lifetimes of excited He_2* molecules are short enough to emit radiation within the observation region. It is therefore reasonable to assume that the relative emission intensities are proportional to their formation rate constants.

In general, the overall rate constant of the production of an upper state of He_2*, $k(u)$, is given by summation of direct formation rate constant, $k_0(u)$, and the contribution of radiative cascade from upper states, $k(u\text{: cascade})$,

$$k(u) = k_0(u) + k(u\text{: cascade}). \qquad (9)$$

Radiative cascade does not contributes to the formation of all excited levels (Table 1). Therefore, the relation $k(u) = k_0(u)$ holds in the formation of 12 or 11 excited states in the $He_2^+/C_6F_6^-$ and $He_2^+/C_6F_5Cl^-$ reactions, respectively.

Table 2 shows excitation energies of observed He_2* states (T_0) and $k_0(u)$ values in the $He_2^+/C_6F_6^-$ and $He_2^+/C_6F_5Cl^-$ reactions. The dependence of $k_0(u)$ on the energy of He_2* state in the $He_2^+/C_6F_6^-$ and $He_2^+/C_6F_5Cl^-$ reactions is shown in Figs. 5 and 6, respectively. The $k_0(u)$ value rapidly decreases with increasing the excitation energy of He_2*. A similar tendency was observed for He* in the $He^+/C_6F_5X^-$(X=F, Cl) neutralization reaction,[19] indicating that ion-ion neutralization dynamics is similar between atomic He^+ and molecular He_2^+ ions. Major triplet and singlet He_2* states

Table 2. Observed triplet and singlet excited states, energies (E_{state}), relative formation rate constants ($k_0(u)$), and equilibrium internuclear distance (r_e) of He_2* excimer.

State	E_{state}	$He_2^+/C_6F_6^-$		$He_2^+/C_6F_5Cl^-$	
	(eV)	$k_0(u)$	R_c(Å)	$k_0(u)$	R_c(Å)
$f^3\Delta_u(3d\delta)$	20.7	1.1	14.9	4.0	14.9
$f^3\Pi_u(3d\pi)$	20.7	1.8	14.0	2.8	14.2
$f^3\Sigma_u^+(3d\sigma)$	20.6	1.7	13.7	2.8	13.9
$e^3\Pi_g(3p\pi)$	20.6	1.0	13.6	1.7	14.2
$d^3\Sigma_u^+(3s\sigma)$	20.5	5.4	12.1	6.7	12.9
$c^3\Sigma_g^+(3p\sigma)$	19.3	100	6.1	100	6.9
$F^1\Delta_u(3d\delta)$	20.7	0.3	19.2	0.6	19.2
$F^1\Pi_u(3d\pi)$	20.7	0.2	17.9	0.6	18.2
$F^1\Sigma_u^+(3d\sigma)$	20.7	0.3	17.3	0.6	17.6
$E^1\Pi_g(3p\pi)$	20.7	0.1	17.2	0.4	18.1
$D^1\Sigma_u^+(3s\sigma)$	20.6	0.2	14.8	0.0	16.0
$C^1\Sigma_g^+(3p\sigma)$	19.6	30.7	6.7	25.5	7.8

were the lowest observed $c^3\Sigma_g^+$ and $C^1\Sigma_g^+$ states, which occupied 70% and 21% of $\sum_u k_0(u)$, in the $He_2^+/C_6F_6^-$ reaction, and 69% and 18% in the $He_2^+/C_6F_5Cl^-$ reaction, respectively. The $k_0(u)$ values of higher d, e, f, D, E, and F states in the $He_2^+/C_6F_6^-$ and $He_2^+/C_6F_5Cl^-$ reactions are smaller than 6.7%, indicating that the formation of these high energy states are unfavorable. The $\sum_u k_0(u)$ value of high energy d, e, f, E, and F states in the $He_2^+/C_6F_5Cl^-$ reaction (20.2%) is larger than d, e, f, D, E, and F states (12.1%) in the $He_2^+/C_6F_6^-$ reaction by a factor of 67%. This suggests that the formation of high energy d, e, f, E, and F states is more favorable in the $He_2^+/C_6F_5Cl^-$ reaction. The total formation ratio of the triplet/singlet states was about 3.5 and 4.3 in the $He_2^+/C_6F_6^-$ and $He_2^+/C_6F_5Cl^-$ reactions, respectively, which were slightly larger than a statistical ratio of 3.0.

3.3 Vibrational distribution of He_2* and rotational distributions of He_2(f, e, d, c, C: $v' = 0$) in the $He_2^+/C_6F_6^-$ and $He_2^+/C_6F_5Cl^-$ reactions

Only (0,0) bands were observed for all the He_2* systems, so that no vibrational excitation was observed. Rotational populations of He_2*

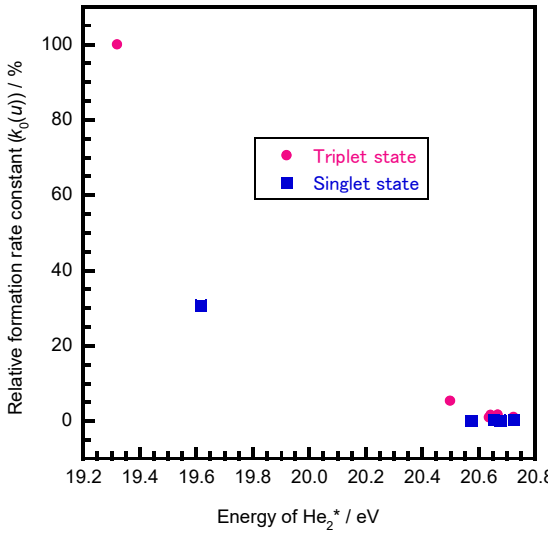

Fig. 5. The dependence of $k_0(u)$ on the energy of He_2* state in the $He_2^+/C_6F_6^-$ reaction.

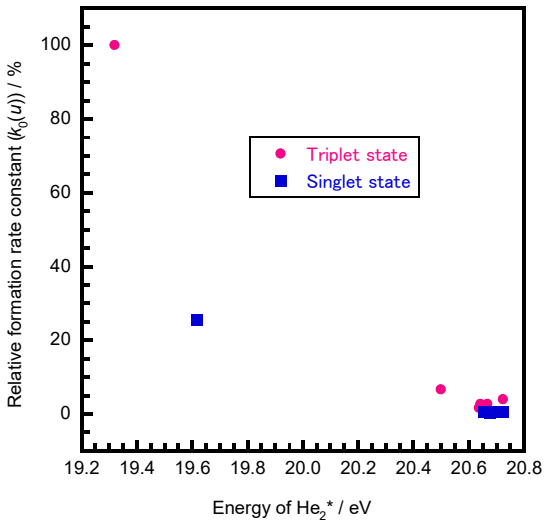

Fig. 6. The dependence of $k_0(u)$ on the energy of He_2* state in the $He_2^+/C_6F_5Cl^-$ reaction.

were estimated for five band systems, for which rotational structures are well resolved. Figures 7a–7d and 8a–8d show expanded emission spectra of the $f^3\Sigma_u^+$-$b^3\Pi_g$, $e^3\Pi_g$-$a^3\Sigma_u^+$, $d^3\Sigma_u^+$-$b^3\Pi_g$, and $c^3\Sigma_g^+$-$a^3\Sigma_u^+$ + $C^1\Sigma_g^+$-$A^1\Sigma_u^+$ systems of He_2* in the $He_2^+/C_6F_6^-$ and $He_2^+/C_6F_5Cl^-$ reactions, respectively. In ^{4}He, the nuclear spin is zero and due to the symmetry rules for homonuclear molecules all even or odd numbered rotational levels are missing.[13-15,25] Therefore, only odd or even levels of P, Q, or R branches are observed in the above five transitions.

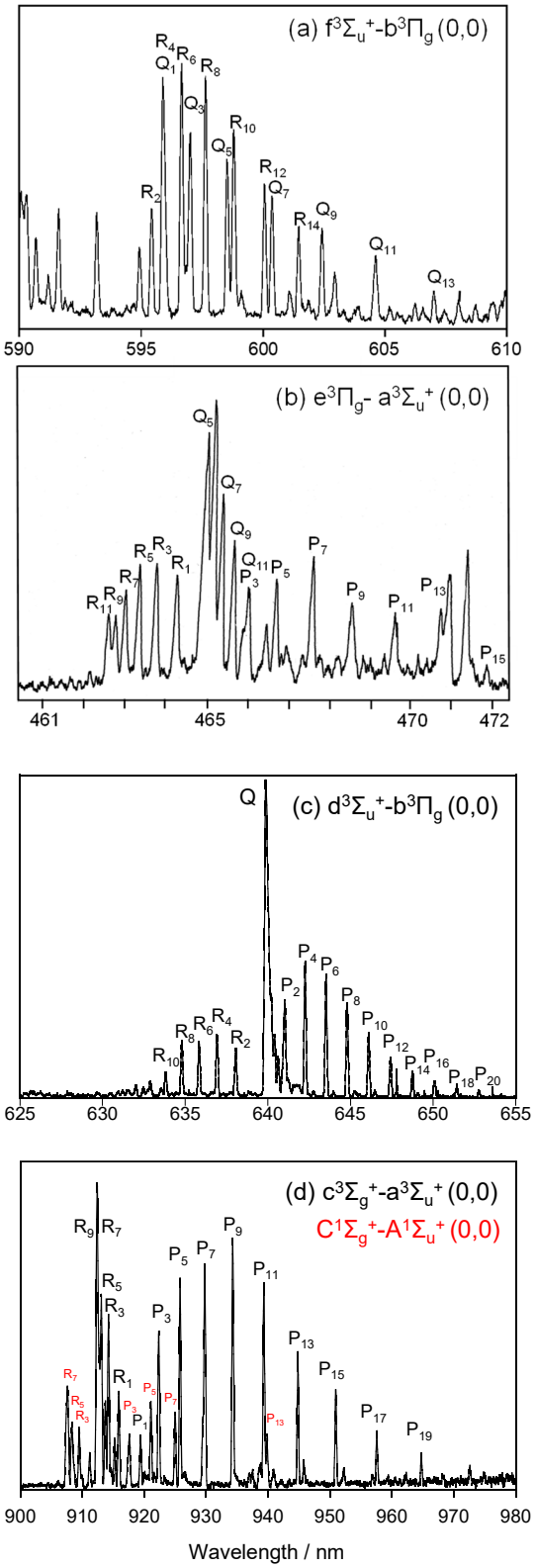

Fig. 7. Rotational structures of the (0,0) bands of He_2(f-b,e-a,d-b,c-a,C-A) systems resulting from the $He_2^+/C_6F_6^-$ reaction in the He FA at a He gas pressure of 1.8 Torr.

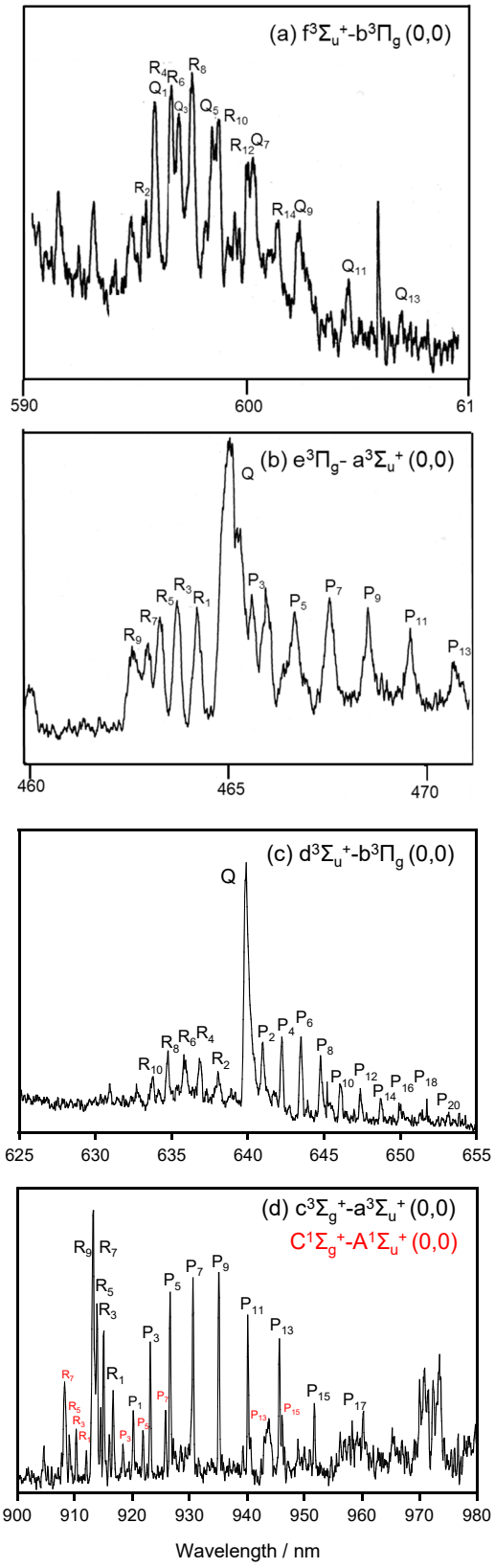

Fig. 8. Rotational structures of the (0,0) bands of He_2(f-b,e-a,d-b,c-a,C-A) systems resulting from the $He_2^+/C_6F_5Cl^-$ reaction in the He FA at a He gas pressure of 1.8 Torr.

Rotational distributions of the f, e, d, c, and C states in the ground vibrational levels were determined from relative intensities of Q or P branch. Rotational levels of He_2* which belong to Hund's case (b) are represented by the quantum number N'. The band intensity (photons s^{-1}) of a transition from a $(v'\,N')$ level to a $(v''N'')$ level is expressed as

$$I_{v'N'v''N''} \propto N_{v'N'}\,Re^2(\bar{r}_{v'v''})q_{v'v''}\nu^3_{v'N'v''N''}S_{N'N''}/g_{N'}, \quad (10)$$

where $N_{v'N'}$ is the rotational population in a given vibrational level, $Re(\bar{r}_{v'v''})$ the electronic transition moment, $q_{v'v''}$ the Franck-Condon factor (FCF), $\nu_{v'N'v''N''}$ the transition frequency, $S_{N'N''}$ the rotational line strength, and $g_{N'} = 2N' + 1$.[25] When a fixed $(v', v")$ band, $Re(\bar{r}_{v'v''})$ and $q_{v'v''}$ values are constant. Assuming a Boltzmann distribution, Boltzmann rotational temperature is obtained from the following relation:

$$\ln\left(\frac{I_{N'N''}}{\nu^3_{N'N''}S_{N'N''}}\right) \propto const - hcB_{v'}N'(N'+1)/kT_{Rot}, \quad (11)$$

where k and T_{Rot} are the Boltzmann constant and the Boltzmann rotational temperature, respectively.[25] In Figs. 9a–9e and 10a–10e, $\ln\left(I_{N'N''}/\nu^3_{N'N''}S_{N'N''}\right)$ values are plotted against $N'(N'+1)$ for the $v' = 0$ levels of the f, e, d, c, and C states in the $He_2^+/C_6F_6^-$ and $He_2^+/C_6F_5Cl^-$ reactions, respectively. Results show that plots can be fitted by either single or double Boltzmann temperatures. From the slopes, $hcB_{v'}/kT_{Rot}$, the effective rotational temperatures, T_{Rot}, are estimated for each state. Results obtained are shown in Table 4. For comparison corresponding data for the $He_2^+/2e^-$ CRR reaction[7] are also shown. The rotational temperature of the f state in the $He_2^+/C_6F_5Cl^-$ reaction is lower than that in the $He_2^+/C_6F_6^-$ reaction. On the other hand, rotational temperatures of the e, d, c, and C states in the $He_2^+/C_6F_5Cl^-$ reaction are higher than or about the same as those in the $He_2^+/C_6F_6^-$ reaction. Rotational temperatures of the f, e, d, and c states in the $He_2^+/C_6F_5X^-$ (X=F, Cl) reactions are higher than those in the $He_2^+/2e^-$ CRR reaction.[7]

From the observed rovibrational distributions of He_2(f, e, d, c, C) in the $He_2^+/C_6F_6^-$ and $He_2^+/C_6F_5Cl^-$ reactions, we estimated the average vibrational and rotational energies of each state, denoted as $<E_v>$ and $<E_r>$, and the average yields of total available energy into these degrees of freedom, denoted as $<f_v>$ and $<f_r>$, respectively. Here, the total available

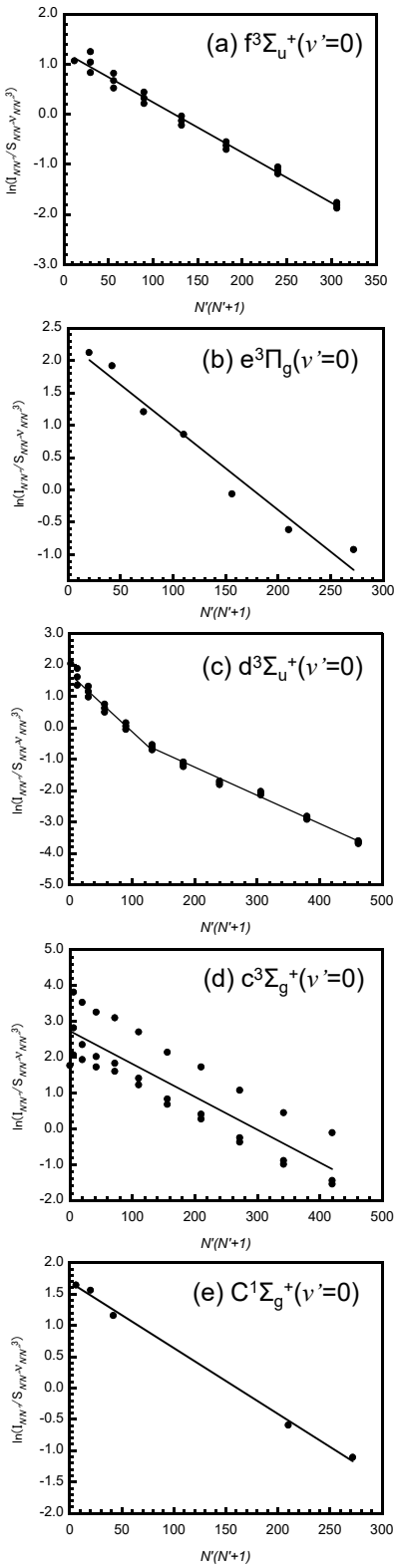

Fig. 9. Estimation of effective rotational temperatures from the slopes of $\ln\left(I_{N'N''}/\nu^3_{N'N''}S_{N'N''}\right)$ against $N'(N'+1)$ for the He_2(f:v'=0), He_2(e:v'=0), He_2(d:v'=0), He_2(c:v'=0), and He_2(C:v'=0) states in the $He_2^+/C_6F_6^-$ reaction.

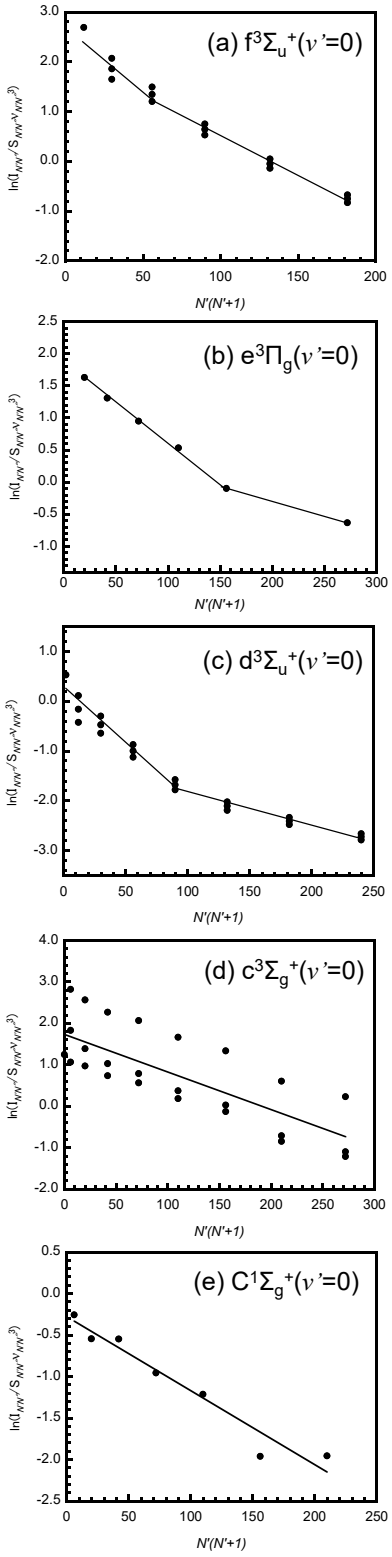

Fig. 10. Estimation of effective rotational temperatures from the slopes of $\ln(I_{N'N''}/\nu_{N'N''}^3 S_{N'N''})$ against $N'(N'+1)$ for the He_2(f:v'=0), He_2(e:v'=0), He_2(d:v'=0), He_2(c:v'=0), and He_2(C:v'=0) states in the $He_2^+/C_6F_5Cl^-$ reaction.

energies for the formation of each He_2^* state were calculated from the relation: $E_{tot} = -\Delta H_0^\circ + 4RT$ at 300 K. From the $\langle E_v \rangle$, $\langle E_r \rangle$, $\langle f_v \rangle$, and $\langle f_r \rangle$ values, the sum of the relative translational energy and internal energy of C_6F_5X, $\langle E_t \rangle + \langle E_{int}(C_6F_5X) \rangle$, and its fraction of the total energy, $\langle f_t \rangle + \langle f_{int}(C_6F_5X) \rangle$, were determined. Results obtained are summarized in Table 5. The $\langle f_r \rangle$ values in the $He_2^+/C_6F_6^-$ and $He_2^+/C_6F_5Cl^-$ reactions are 2.8–9.6% and 3.1–9.6%, respectively. The $\langle f_v \rangle$ values are zero for both reactions. Although the E_{tot} values for the low energy c and C states are larger than those of higher f, e, and d states, their $\langle E_r \rangle$ values are similar to those of the upper three states. Therefore, the $\langle f_r \rangle$ values of the c and C states are smaller than those of upper three states. Thus, $\langle f_t \rangle + \langle f_{int}(C_6F_5X) \rangle$ values of the c and C states are slightly larger than those of upper states. On the basis of $\langle f_t \rangle + \langle f_{int}(C_6F_5X) \rangle$ values, most of the total available energies (90.4–97.2%) are deposited into relative translational energies of $He_2^* + C_6F_5X$ (X=F, Cl) products and internal energies of C_6F_5X. Among three internal energy (electronic, vibrational, and rotational energies), electronic energy can be excluded from an acceptor mode of excess energies, because the energies of $C_6F_5X^*$ (S_1) states (>4 eV)[22,26] are higher than excess energies released in processes (7a) and (8a). Therefore, C_6F_5X accepts excess energies as their vibrational and rotational energies in the ground electronic states.

3.3 Reaction dynamics of the $He_2^+/C_6F_6^-$ and $He_2^+/C_6F_5Cl^-$ neutralization reactions

Since the formation of He_2^* takes place via strongly attractive ion–pair potentials, a long lived $[He_2–C_6F_5X]^*$ complex can be postulated:

$$He_2^+ + C_6F_5X^- \rightarrow [He_2–C_6F_5X]^* \rightarrow He_2^* + C_6F_5X. \quad (8)$$

According to a simple statistical theory,[27–29] the vibrational and rotational prior populations of a given He_2^* level are given by the relations:

$$P^o(v') \propto (E_{\mathrm{tot}} - E_{v'})^{33}, \quad (9)$$

$$P^o(N') \propto (2N'+1)(E_{\mathrm{tot}} - E_{N'})^{32}. \quad (10)$$

The prior vibrational distributions of v'=0–3 levels of He_2(f, e, d, c, C) states were calculated as follow:

Table 4. Rotational temperatures of He_2(f, e, d, c, C) produced from the $He_2^+/C_6F_6^-$ and $He_2^+/C_6F_5Cl^-$ reactions and $He_2^+/2e^-$ CRR reaction.

Emitting species	$He_2^+/C_6F_6^-$ T_r/ K	$He_2^+/C_6F_5Cl^-$ T_r/ K	$He_2^+/2e^{-a)}$ T_r/ K
$He_2(f^3\Sigma_u^+: v'=0)$	1020±20	620±30	580±20 (N'=5–13)
		350±50	310±70 (N'=1–5)
$He_2(e^3\Pi_g: v'=0)$	770±60	2150	990±190 (N'=10–16)
		800±20	500±20 (N'=2–10)
$He_2(d^3\Sigma_u^+: v'=0)$	1170±30	1530±110	830±20 (N'=7–17)
	530±30	470±40	440±50 (N'=1–7)
$He_2(c^3\Sigma_g^+: v'=0)$	1080±110	1090±180	720±140 (N'=0–12)
$He_2(C^1\Sigma_g^+: v'=0)$	940±30	1110±120	

a) Ref. 7.

Table 5. Total available energy, average vibrational and rotational energies deposited into He_2(f, e, d, c, C), and average fractions of vibrational and rotational energies of He_2(f, e, d, c, C) and relative translational energies + internal energies of C_6F_5X deposited in the He_2^+/C_6F_5X (X=F, Cl) reactions.

Reaction	State	E_{tot} (eV)	$<E_r>$ (eV)	$<E_v>$ (eV)	$<f_r>$ (%)	$<f_v>$ (%)	$<f_v>+<f_r>$ (%)	$<f_t>+<f_{int}(C_6F_5X)>$ (%)
$He_2^+/C_6F_6^-$	$f^3\Sigma_u^+$	1.15	0.11	0.0	9.6	0.0	9.6	90.4
	$e^3\Pi_g$	1.16	0.07	0.0	6.0	0.0	6.0	94.0
	$d^3\Sigma_u^+$	1.30	0.07	0.0	5.4	0.0	5.4	94.6
	$c^3\Sigma_g^+$	2.48	0.07	0.0	2.8	0.0	2.8	97.2
	$C^1\Sigma_g^+$	2.18	0.08	0.0	3.7	0.0	3.7	96.3
$He_2^+/C_6F_5Cl^-$	$f^3\Sigma_u^+$	0.93	0.04	0.0	4.3	0.0	4.3	95.7
	$e^3\Pi_g$	0.94	0.09	0.0	9.6	0.0	9.6	90.4
	$d^3\Sigma_u^+$	1.08	0.06	0.0	5.6	0.0	5.6	94.4
	$c^3\Sigma_g^+$	2.26	0.07	0.0	3.1	0.0	3.1	96.9
	$C^1\Sigma_g^+$	1.96	0.08	0.0	4.1	0.0	4.1	95.9

$He_2^+/C_6F_6^-$

He_2(f: v'=0–2) = 1.0 : 2.5(-03) : 2.6(-06),
He_2(e: v'=0–2) = 1.0 : 1.6(-03) : 8.3(-07),
He_2(d: v'=0–2) = 1.0 : 2.0(-03) : 2.9(-06),
He_2(c: v'=0–2) = 1.0 : 7.9(-02) : 6.2(-03),
He_2(C: v'=0–2) = 1.0 : 4.5(-02) : 1.8(-03),

$He_2^+/C_6F_5Cl^-$

He_2(f: v'=0–2) = 1.0 : 5.1(-04) : 5.1(-08),
He_2(e: v'=0–2) = 1.0 : 3.0(-04) : 1.1(-08),
He_2(d: v'=0–2) = 1.0 : 9.4(-04) : 2.1(-07),
He_2(c: v'=0–2) = 1.0 : 6.1(-02) : 3.6(-03),
He_2(C: v'=0–2) = 1.0 : 3.1(-02) : 8.2(-04),

where (n) is power of 10 multiplying the entry. The prior vibrational distributions predict low vibrational excitation, which is consistent with the experimental observations.

Figures 11a–11e and 12a–12e show observed and prior rotational distributions of the f, e, d, c, and C states in the $He_2^+/C_6F_6^-$ and $He_2^+/C_6F_5Cl^-$ reactions, respectively. Observed rotational distributions of $f^3\Sigma_u^+(v'=0)$ and $e^3\Pi_g(v'=0)$ in the $He_2^+/C_6F_6^-$ reaction and $e^3\Pi_g$ (v' =0) and $C^1\Sigma_g^+(v'=0)$ in the $He_2^+/C_6F_5Cl^-$ reaction are higher than prior ones. On the other hand,

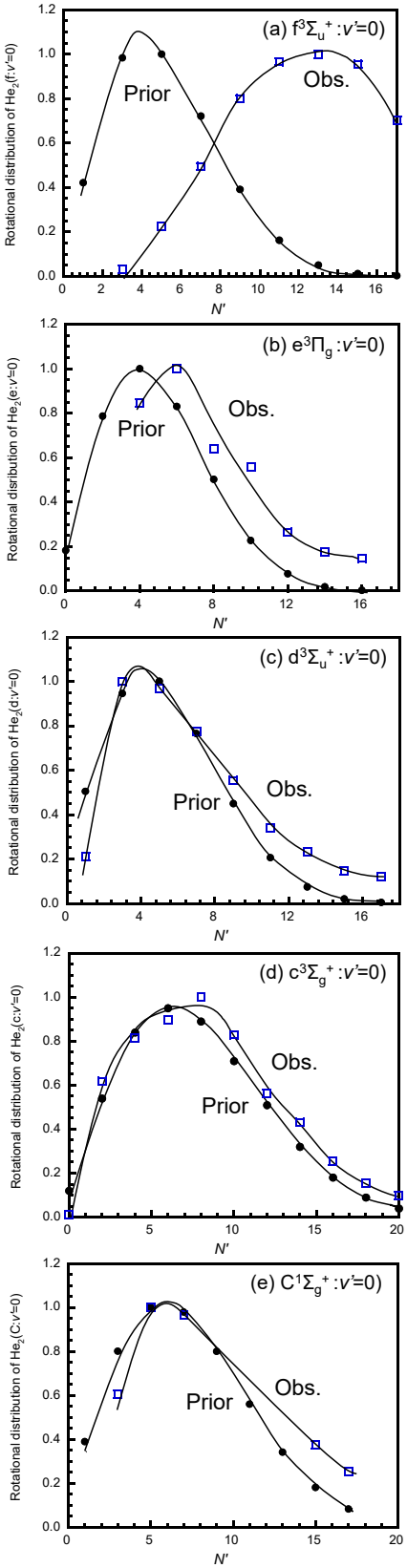

Fig. 11. Observed and statistical prior rotational distributions of the He_2(f: v'=0), He_2(e: v'=0), He_2(d: v'=0), He_2(c: v'=0), and He_2(C: v'=0) states in the $He_2^+/C_6F_6^-$ reaction.

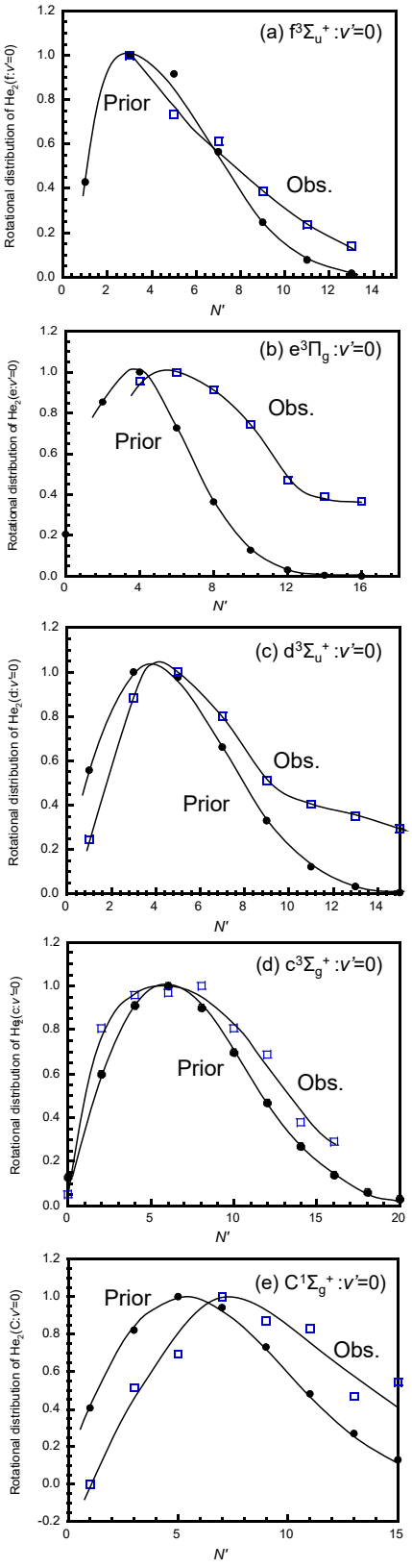

Fig. 12. Observed and statistical prior rotational distributions of the He_2(f: v'=0), He_2(e: v'=0), He_2(d: v'=0), He_2(c: v'=0), and He_2(C: v' =0) states in the $He_2^+/C_6F_5Cl^-$ reaction.

observed rotational distributions are in reasonable agreement with the prior ones for $d^3\Sigma_u^+(v'=0)$, $c^3\Sigma_g^+(v'=0)$, and $C^1\Sigma_g^+(v'=0)$ in the $He_2^+/C_6F_6^-$ reaction and $f^3\Sigma_u^+(v'=0)$, $d^3\Sigma_u^+(v'=0)$, and $c^3\Sigma_g^+(v'=0)$ in the $He_2^+/C_6F_5Cl^-$ reaction. Therefore, long-lived $[He_2–C_6F_5X]^*$ intermediates take part in the formation of many He_2^* states in the $He_2^+/C_6F_6^-$ and $He_2^+/C_6F_5Cl^-$ reactions.

The ion–ion neutralization reactions studied here proceed through strongly attractive $V[He_2^+,C_6F_5X^-]$ ion-pair potentials. He_2^* arises from diversion of trajectories from the entrance $V[He_2^+,C_6F_5X^-]$ potential to the exit $V[He_2^*,C_6F_5X]$ potentials due to a strong coupling between the two potentials. Thus the electronic state distribution of He_2^* reflects the different crossing point of the strongly attractive ion-pair entrance potentials and rather flat covalent exit potentials at the crossing points and the coupling between each pair of states. The $He_2^+–C_6F_5X^-$ separations at crossing points R_c are calculated from the relation:

$$R_c = e^2/(\mathrm{IP}–\mathrm{EA}) = 14.40/(\mathrm{IP}–\mathrm{EA}), \qquad (11)$$

where IP is the ionization potential of He_2^* and EA is the electron affinity of C_6F_5X. The R_c values for the formation of each He_2^* state are calculated for each reaction. The results are given in Table 2.

The ion–ion neutralization reactions proceed through an approach of the He_2^+ and $C_6F_5X^-$ ion pair under their mutual Coulombic field followed by an electron transfer from $C_6F_5X^-$ to He_2^+. Since the Born–Oppenheimer approximation holds during a fast electron transfer, the relative motion of an ion pair is unchanged after the neutralization. Therefore, a large kinetic energy resulting from the strong mutual Coulombic force is conserved at the instant of electron transfer. The electron transfer occurs at relatively large intermolecular separations of 6.1–19.2 Å, where interactions between neutral He_2^* and C_6F_5X molecules are small. Thus, a large amount of the kinetic energy will remain in the neutral products.

Under the Born–Oppenheimer approximation, the internuclear separations of He_2^+ ions are unchanged just after the neutralization. Since the equilibrium nuclear separation of He_2^+ ($X^2\Sigma_u^+$:1.081 Å) is close to those of He_2^*(1.068–1.097 Å for f, e, d, c, F, E, D, and C states),[12] the formation of He_2^* with the largest FCFs for the $He_2^+(X: v'' = 0) \rightarrow He_2^*$(f, e, d, c, and C: $: v' = 0$) neutralization will be most favorable, as evaluated in the previous paper.[7] This prediction is consistent with the preferential formation of He_2^*(f, e, d, c, and C) in the $v' = 0$ levels."

Just after the neutralization the geometries of $C_6F_5X^-$ (X= F, Cl) anions are also reserved. Structural information on the geometries of C_6F_5X has been obtained from theoretical calculations by Miller et al.[10,11] using the GAUSSIAN-03 program.[30] According to their calculations, aromatic neutral C_6F_6 molecule is obviously completely planar with D_{6h} symmetry. On the other hand, the calculated $C_6F_6^-$ anion structure is non-planar with C_{2v} symmetry, where two opposite F atoms protrude above the average carbon plane by about 23°. The C atoms to which these two F atoms are bound lie very slightly below the plane in which the remaining four C atoms lie, with a dihedral angle of −0.5°. The remaining four F atoms lie in a plane of their own, slightly below that of the four planar C atoms. A symmetry change is also observed between C_6F_5Cl and its anion from C_{2v} to C_s, resulting in a change in the rotational symmetry number from 2 to 1. C_6F_5Cl is a planar molecule, whereas $C_6F_5Cl^-$ is a non-planar anion where Cl atom protrudes above the average carbon plane by about 21.3° (B3LYP/6-311+G(3df) optimizations) or 37.1° (G3(MP2) calculation).

Since the equilibrium geometries of $C_6F_5X^-$ are significantly different from those of C_6F_5X, some energy will be released as the vibrational energy of C_6F_5X after the neutralization reaction. Consequently, most of excess energies will be transformed into the vibrational energy of C_6F_5X and the relative kinetic energy of the neutral products in the $He_2^+/C_6F_5X^-$ neutralization reactions.

4. Summary and Conclusion

The ion-ion neutralization reactions of He_2^+ with $C_6F_6^-$ and $C_6F_5Cl^-$ were studied by observing He_2^* excimer emissions in the He FA. Six triplet and six or five singlet transitions of He_2^* with excitation energies of 19.3–20.7 eV were identified. Major triplet and singlet He_2^* states were the lowest observed $c^3\Sigma_g^+$ and $C^1\Sigma_g^+$ states, which occupied 70% and 21% of $\sum_u k_0(u)$, in the $He_2^+/C_6F_6^-$ reaction, and 69% and 18% in the $He_2^+/C_6F_5Cl^-$ reactions, respectively. Thus the k_0 ($c^3\Sigma_g^+$) + k_0 ($C^1\Sigma_g^+$) values occupy 91% and 87% of $\sum_u k_0(u)$ in the $He_2^+/C_6F_6^-$ and $He_2^+/C_6F_5Cl^-$ reactions,

respectively. The total formation ratio of the triplet/singlet states was about 3.5 and 4.3 in the $He_2^+/C_6F_6^-$ and $He_2^+/C_6F_5Cl^-$ reactions, which were slightly larger than a statistical ratio of 3.0. No vibrational excitation was observed for all observed He_2^* states because of large FCFs for $He_2^+(X: v'' = 0) \rightarrow He_2^*(f, e, d, c,$ and $C: v' = 0)$ neutralization. The rotational distributions of $f^3\Sigma_u^+$ ($v' = 0$), $e^3\Pi_g$ ($v' = 0$), $d^3\Sigma_u^+(v'=0)$, $c^3\Sigma_g^+(v'=0)$, and $C^1\Sigma_g^+(v'=0)$ states were expressed by either single or double Boltzmann rotational temperatures of 310–1530 K. Rovibrational distributions of these excited states indicated that most of excess energies are not released as rovibrational energies of He_2^* but they (90.4–97.2%) are deposited into rovibrational energies of C_6F_5X (X=F, Cl) and relative translational energies of products. Equilibrium molecular structures of C_6F_5X are planer, whereas those of $C_6F_5X^-$ anions are non-planer. Therefore, vibrational energies of C_6F_5X are the most important internal energy of C_6F_5X. The observed vibrational and rotational distributions were compared with statistical ones assuming long lived $[He_2–C_6F_5X]^*$ intermediates. In many cases, a reasonable agreement between observed and prior vibrational and rotational distributions were found. Therefore it was concluded that long lived $[He_2–C_6F_5X]^*$ intermediates take part in most of the neutralization reactions.

Acknowledgments

The authors acknowledge Prof. Kenji Furuya of Kyushu University for his careful reading of our manuscript. This work has been supported by the Mitsubishi foundation (1996).

References

1) D. R. Bates, A. E. Kingston, and R. W. P. McWhirter, *Proc. R. Soc., Ser. A*, 267, 297 (1962).
2) M. R. Flannery, *Adv. At, Mol. Opt. Phys.*, 32, 117 (1994).
3) M. R. Flannery, in "*Handbook of Atomic, Molecular, and Optical Physics*", 800, Edited by G. Drake, Springer, New York (2006).
4) N. G. Adams, V. Poterya, and L. M. Babcock, *Mass Spectrom. Rev.*, 25, 798 (2006).
5) M. Tsuji, in "*Advances in Gas-Phase Ion Chemistry*" *Vol. 4.*, Edited by N. G. Adams and L. M. Babcock, Elsevier, 137 (2001).
6) Z. Liu, M. Roy, N. J. DeYonker, and R. Gopalakrishnan, *J. Chem. Phys.*, 159, 114111 (2023).
7) M. Tsuji and E. Oda-Sako, *Eng. Sci. Rep. Kyushu Univ.*, 45, 1 (2024).
8) M. Tsuji, E. Oda, M. Tanaka, M. Nakamura, and Y. Nishimura, *Chem. Lett.*, 26, 465 (1997).
9) Y. Ikezoe, S. Matsuoka, M. Takebe, and A. Viggiano, "*Gas Phase Ion-Molecule Reaction Rate Constants through 1986*", Maruzen, Tokyo (1987).
10) T. M. Miller, J. M. Van Doren, A. A. Viggiano, *Int. J. Mass Spectrom.*, 233, 67 (2004).
11) T. M. Miller and A. A. Viggiano, *Phys. Rev. A*, 71, 012702 (2005).
12) K. P. Huber and G. Herzberg, "*Molecular Spectra and Molecular Structure, IV. Constants of Diatomic Molecules*", Van Nostrand Reinhold, New York (1979).
13) M. L. Ginter, *J. Chem. Phys.*, 42, 561 (1965).
14) M. L. Ginter, *J. Mol. Spectrosc.*, 18, 321 (1965).
15) C. M. Brown and M. L. Ginter, *J. Mol. Spectrosc.*, 40, 302 (1971).
16) M. Allan and J.P. Maier, *Chem. Phys. Lett.*, 34, 442 (1975).
17) J. P. Maier, O. Marthaler, M. Mohraz, and R. H. Shiley, *Chem. Phys.*, 47 295 (1980).
18) *Atomic Spectra Database*, *NIST Standard Reference Database*, 78, Ver. 5.9. Oct. (2021).
19) M. Tsuji, M. Nakamura, Y. Nishimura, E. Oda, H. Oota, and M. Hisano, *J. Chem. Phys.*, 110, 2903 (1999).
20) M. Tsuji, M. Nakamura, and Y. Nishimura, *Chem. Lett.*, 26, 259 (1997).
21) S. Yamaguchi, M. Tsuji, and Y. Nishimura, *J. Chem. Phys.*, 88, 3111 (1988).
22) *NIST Chemistry WebBook, NIST Standard Reference Database*, Number 69 (2023) https://doi.org/10.18434/T4D303.
23) Y.-R. Luo, "*Bond Dissociation Energies*", Number 69 in *CRC Handbook of Chemistry and Physics*, 81th Ed., CRC Press, Boca Raton (2000).
24) S. Neeser, R. Tietz, M. Schulz, and H. Langhoff, *Z. Phys. D.*, 31, 61 (1994).
25) G. Herzberg, "*Molecular Spectra and Molecular Structure: I. Spectra of Diatomic Molecules*", 2nd ed. Van Nostrand Reinhold, New York (1950).
26) M. Z. Zgierski, T. Fujiwara, and E. C. Lim, *J. Chem. Phys.,* 122, 144312 (2005).
27) R. D. Levine, *Annu. Rev. Phys. Chem.*, 29, 59 (1978).
28) R. D. Levine and J. L. Kinsey, in "*Atom–Molecule Collision Theory*", Edited by R. B. Bernstein, Plenum, New York, (1979).
29) E. Zamir and R. D. Levine, *Chem. Phys.*, 52, 253 (1980).
30) M. J. Frisch *et al.*, "*GAUSSIAN 03*", *Revision B.02*, Gaussian, Inc., Pittsburgh, (2003).